University of Ljubljana

Faculty of Mathematics and Physics

Understanding and reproducing the Gecko adhesive system

Author: Domen Rozman

Supervisor: Rudolf Podgornik

March 7th, 2012

1. Abstract

Gecko lizards have evolved one of the most effective adhesives known to man enabling them to effortlessly run on vertical and even inverted surfaces. Lamellae on a gecko's toe pad host a complex array of 30-120μm long fibres from ß-keratin that each branch out in to hundreds of nano-structures. When a gecko makes a step millions of these nano-structures make intimate contact with the surface insuring a strong load dependant adhesive bond by way of Van der Waals forces. Understanding the Gecko adhesion system on all size scales enables us to effectively model and evolve synthetic dry adhesives with Gecko like functional properties.

2. Contents

3. Introduction

The extraordinary adhesive properties of gecko lizards have been amazing scientists ever since Aristotle first mentioned the animal's extraordinary ability to run up and down a tree in any direction even with its head facing downwards. Gecko toe pads operate in perhaps one of the most sever conditions of any adhesive application. Geckos are capable of attaching and detaching their adhesive toe pads in milliseconds while running with speeds of up to 20 body lengths per second on vertical and even inverted surfaces. Even more fascinating is the fact that they can pull of this extraordinary feat of agility on practically any surface, dry or wet, including glass which has a very smooth surface on a molecular level. Furthermore gecko toe pads are self cleaning, do not self adhere to each other, are not sticky when touched and even adhere to surfaces in complete vacuum.

Over the years many theories have appeared trying to explain how the Gecko adhesive system works. At least 7 different mechanisms have been discussed in the past 175 years. Sticky secretions were ruled out early since toe pads lack glandular tissue. The idea that toe pads act as suction cups was ruled out in 1934 by experiments done in vacuum. Electrostatic attraction forces also seemed not to be at work since geckos could still adhere to metal in ionised air. Micro interlocking was also studied but the theory was challenged by the fact that Geckos can adhere while inverted on finely polished glass. In the late 1960s a set of experiments revealed the fact that surface energy of the substrate, rather than its texture, determined the strength of the attachment implying that intermolecular forces were responsible for Gecko adhesion. The theory that capillary forces are at play remained a strong contender until in 2002 when Autumn and Peattie showed that a strand of Gecko seta made of ß-keratin, a hydrophobic material, can adhere to a plate of hydrophobic but polarisable GaAs. There is only one mechanism that can cause 2 hydrophobic surfaces to adhere in air and that is the Van der Waals force.

The fact that Van der Waals forces are responsible for Gecko adhesion was a big milestone in the research field of dry adhesives. Though to fully understand and be able to reproduce functional properties of gecko adhesion in synthetical adhesives we have to study the Gecko adhesion system as a whole. There are important lessons to be learned at the macro, micro and nano levels of the system. In my seminar I will cover the main discoveries at different size scales, I will move on to explain why synthetical dry adhesives can play a big role in the future of adhesive technology and present a few existing gecko inspired synthetical adhesives.

4. Structural build of a gecko toe pad

On the underside of a gecko's foot expanded digital pads called scansors or scansor pads are lined in rows of lamellae. In the early 1900s using a conventional light microscope scientist discovered that these lamellae are covered with millions of hair like microstructures called setal branches. A single steal branch of a tokay Gecko is approximately 110μm long and 4,2 μm in diameter. Seta are similarly oriented and uniformly distributed on the scansor pads. More than 60 years later using electron scanning microscopes scientists discovered setal branches have split ends and a spatular nanostructure. There are from 100 up to 1000 nano-structures at the end of each setal branch known as spatula. A single spatula consists of a stalk with a thin roughly triangular end that is approximately 0,2 μm in width at the tip.

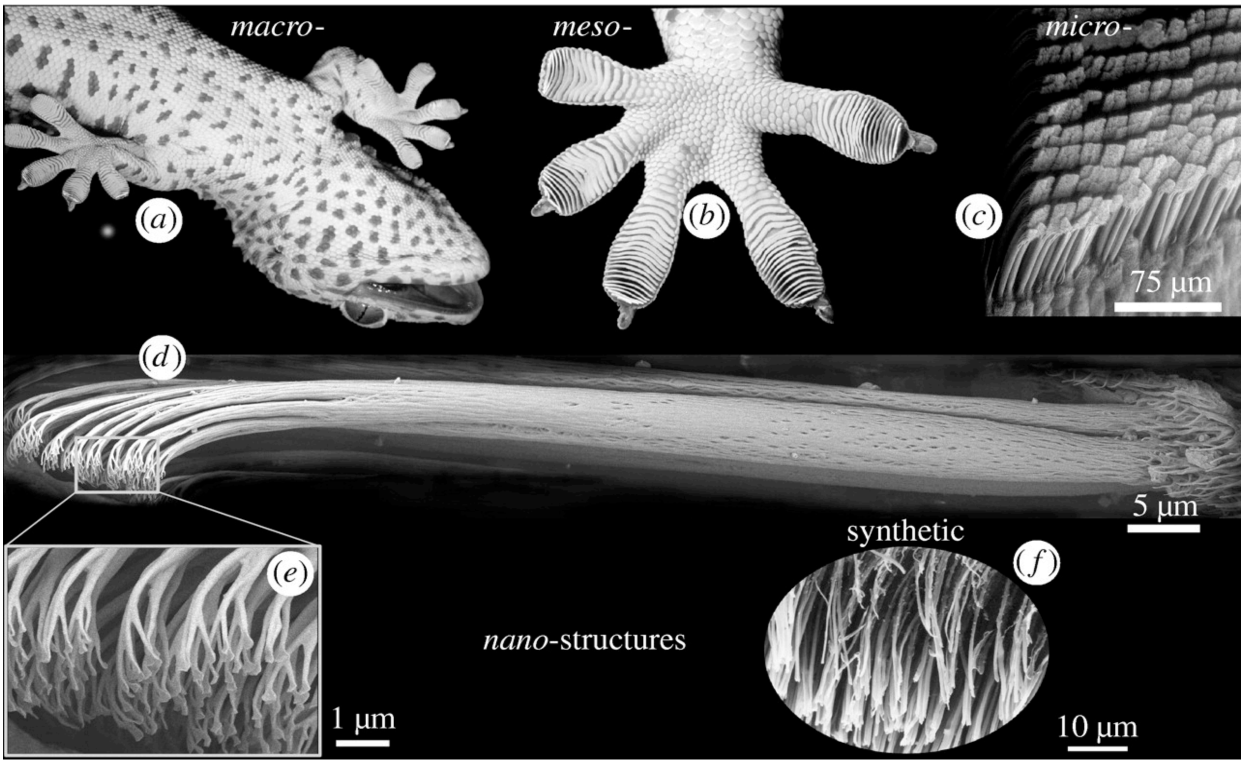 (1)

Structural hierarchy of the gecko adhesive system. (a) Ventral view of a tokay gecko climbing a vertical glass surface. (b) Ventral view of the foot of a tokay gecko, showing a mesoscale array of seta-bearing scansors (c) Microscale array of setae are arranged in a nearly grid-like pattern on the ventral surface of each scansor. (d) Cryo-SEM image of a single gecko seta. (e) Nanoscale array of hundreds of spatular tips of a single gecko seta. (f) Synthetic spatulae fabricated from polyimide at UC Berkeley. [6]

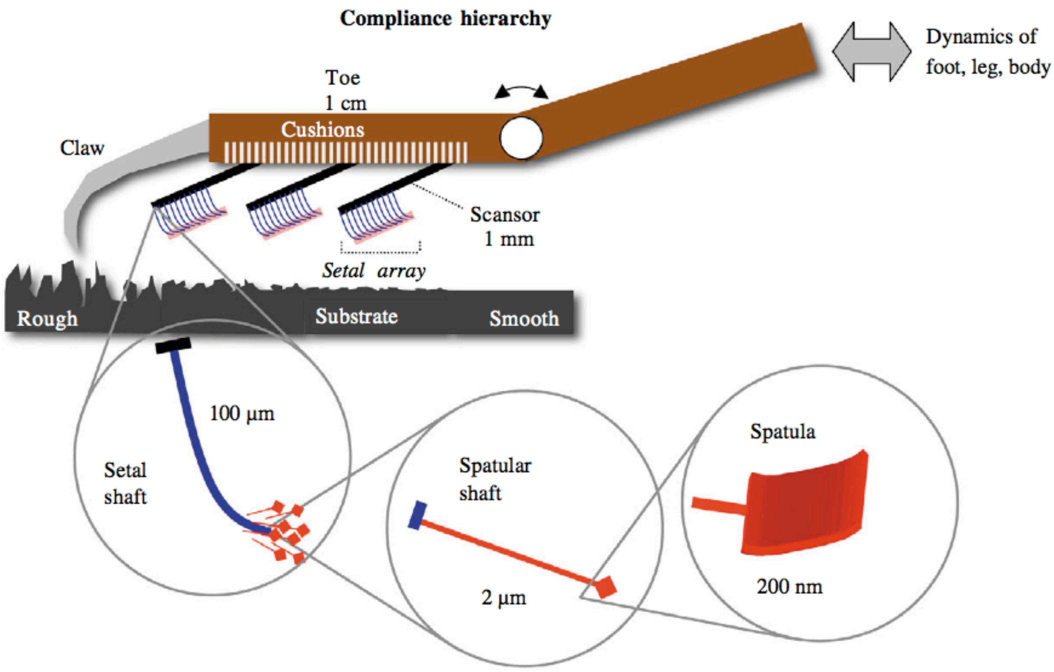 (2)

Schematic of complience hierachy of the Gecko adhesive system. [7]

5. Seven benchmark properties of the Gecko adhesive system

We can break down the functionality of the gecko adhesive system in to 7 main properties. Designers of nano-adhesives use these benchmarks to test how their new synthetic designs measure up to a real gecko toe pad. Understanding the fundamental principles serving each functional property is key. Only then can we develop effective mechanical models that are the basis for designing and understanding synthetic nano-adhesives. In this chapter I will list the 7 functional benchmark properties and explain the underlying physical principles behind each of them. I will start at the molecular level and work my way up.

5.1. Material independence

A single spatula attaches to the surface by Van der Waals forces.

The Van der Waals interaction between the individual spatulae and the surface of the substrate are the reason that gecko adhesion is material independent. The Van der Waals force is the sum of attractive or repulsive forces between molecules other than those due to covalent bonds or to the electrostatic interaction of ions with one another or with natural molecules. [2] We can break it down in to 3 components. The force between two permanent dipoles know as the Keesom force, the force between a permanent dipole and a corresponding induced dipole also know as Debeye force and the force between fluctuating dipoles also known as the London dispersion force. The London dispersion force is a weak intermolecular force arising from quantum induced instantaneous polarization multipoles in molecules. They can therefore act between molecules without permanent multipole moments. This is frequently described as formation of "instantaneous dipoles" that attract each other. London forces are present between all chemical groups and usually represent the main part of the total interaction force in condensed matter. [3]

For Van der Waals interactions between macroscopic bodies we have to sum all of these 3 components. The London interaction is usually the strongest of the 3 because it is always present between all molecules and atoms. All 3 interaction potentials fall with R to the negative power of 6. Thus we can approximate the potential energy as show in equation (3) where A is a material dependant constant.

$$W_{vdW}(r) = W_{Debeye}(r) + W_{Keesom}(r) + W_{london}(r) = -\frac{A}{r^6} \tag{3}$$

For macroscopic bodies with known volumes and numbers of molecules per unit volume, the total Van der Waals force can be computed based on the "microscopic theory" as the sum over all interacting pairs. [2] We are interested in approximating the force with which one spatula is attracted to the substrate. Lets start of with calculating the Van der Waals force between 1 molecule and a solid wall.

As shown in figure (4) we slice the wall in to thin rings. Each infinitesimal ring has a volume dV and dN molecules according to dN = ρdV where ρ is the molecular density of the wall.

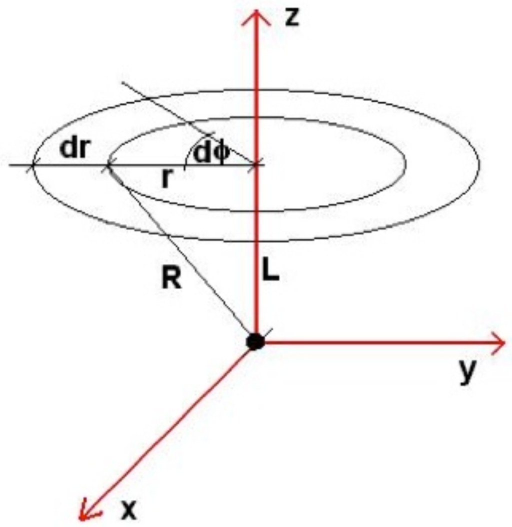

(4)

Schematic drawing of slicing the wall in to thin rings. [15]

Integrating equation (3) over dN and using polar coordinates we calculate the following result.

$$\begin{aligned} W(D) &= \int -\frac{A}{D^6} dN; \quad dN = 2\pi r \rho dr dz \\ &= -2\pi\rho A \int_0^\infty \frac{r dr}{(x^2+z^2)^3} \int_D^\infty dz \\ &= -\frac{\pi\rho A}{6D^3} \end{aligned} \tag{5}$$

We calculate the force between the molecule and the surface as seen in equation (6).

$$F(D) = \frac{\partial W(D)}{\partial D} = \frac{\pi\rho A}{2D^4} \tag{6}$$

We can model individual spatulae as cylinders with a hemispherical end of radius R at the end. [1] In our model we will approximate the force between the spatula and the wall by calculating the force between the spherical end cap of the spatula and the wall. To calculate this attractive force we must integrate equation (5) over all the molecules in the spherical cap.

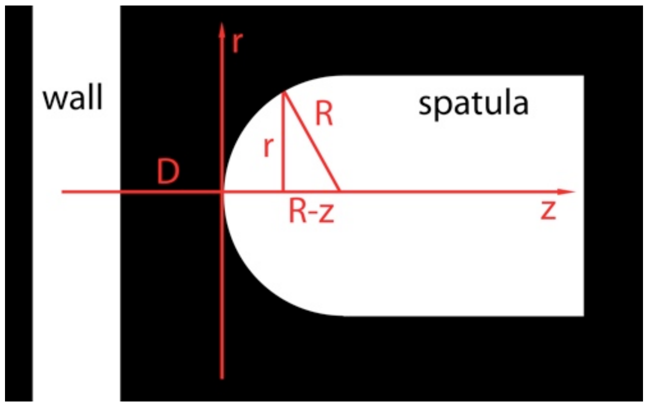

(7)

Model of the spatula as a cylynder with a spherical endcap.

We place the coordinate centre at the peak of the sphere and observe that it is positioned length D away from the wall. As shown in figure (7) all the molecules on a disc with radius r are at length (D + z) from the wall. We calculate the number of molecules in equation (8).

$$dN = \rho_{spatula} \pi r^2 dz \tag{8}$$

Integrating over all of the discs that make up the spherical end cap of the spatula we calculate the total attraction energy as:

$$\begin{aligned} W(D) &= \int W(D+z) dN \\ &= -\int \frac{\pi \rho_{wall} A}{6(D+z)^3} dN \\ &= -\frac{A \rho_{spatula} \rho_{wall} \pi^2}{6} \int_0^R \frac{z(2R-z)}{(D+z)^3} dz \\ &= -\frac{A \rho_{spatula} \rho_{wall} \pi^2}{6} \left(\frac{R}{D} - \frac{1}{2} - \frac{L(D+2R)}{2(D+R)^2} + ln \frac{D}{D+R}\right) \end{aligned} \tag{9}$$

If R >> L and in our case it is we can simplify equation (9) as follows: (10)

$$W(D) \approx -\frac{A\pi^2 \rho_{wall}\rho_{spatula}}{6}\frac{R}{L}$$

As we did in equation (4) we now calculate the force between the spatula and the wall

$$F_{spatula-wall}(D) = \frac{\partial W_{spatula(D)}}{\partial L} = \frac{H_{spatula-wall}R}{6L^2} \quad (11)$$

$$H_{spatula-wall} = A\pi^2 \rho_{spatula}\rho_{wall} \quad (12)$$

In equation (11) we have also introduced the Hamaker constant defined in figure (12). We can see it is material dependant as both the underlying characteristics that define A as well as the spatular and wall molecule densities define its value.

We can now calculate the total adhesive force a Gecko lizard could produce in ideal conditions as follows. A Tokay gecko foot has approximately 230mm^2 of area and a density of 14400 setae/mm^2. Each seta branches out in to 100 - 1000 spatular tips. [4] We calculate the total number of spatular tip contacts with the surface is approximately 1,6 x 10^9.

Spatular tips have a radius of R = 200nm and while adhering we can say they are spaced approximately D = 0,3nm from the surface [5]. The Hamaker constant for ß-keratin is H=10^{-19}J. [5] Using equation (9) we calculate each spatula produces an adhesive force of 0,04μN. The total adhesive force a 50g Gecko could theoretically produce is hence 64N.

The calculated adhesive force of the Gecko setal array is as shown the sum of mostly London dispersion forces between molecules in individual spatulae and the surface. As London dispersion forces work amongst all molecules the strong adhesion that setal arrays produce is material independent.

5.2. Self - cleaning

Small particles rather adhere to the substrate than to one or more spatulae.

How geckos manage to keep their feet clean while walking about with sticky toes has long remained a puzzle. Geckos with dirty feet recovered their ability to cling to vertical surfaces after only a few steps. Setal arrays are the first adhesive that has shown a self-cleaning capability. As shown in figure (13) contact mechanical models that use principles similar to the ones we used to calculate the force of a single spatula to the wall suggest that self-cleaning occurs by an energetic disequilibrium between the adhesive forces attracting a dirt particle to the substrate and those attracting the same particle to one or more spatulae. [4]

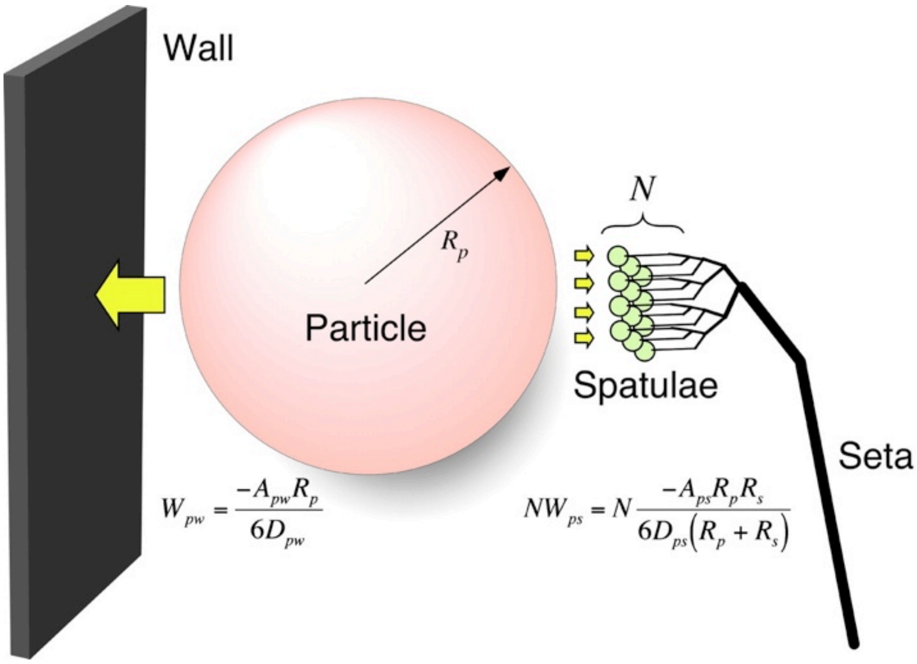

(13) Model of interactions between N gecko spatulae of radius R_s, a spherical dirt particle of radius R_p, and a planar wall. Van der Waals interaction energies for the particle-spatula (W_{ps}) and particle-wall (W_{pw}) systems are shown. When N x W_{ps} = W_{pw}, equal energy is required to detach the particle from wall or N spatulae. Our results suggest that N is sufficiently great that self-cleaning results from energetic dsequilibrium between the wall and the relatively few spatulae that can attach to a single particle. [4]

With the system in energetic equilibrium 50% of the dirt particles attached to a setal array stay on the surface with each step. Models suggest that for self-cleaning to occur in a setal arrays 3 conditions have to be met. (i) The surface of individual spatulae has to be smaller than those of common dirt particles, (ii) spatulae have to be made of relatively hard non-tacky material, (iii) surface energies of materials used have to be kept relatively low. [4]

5.3. Anisotropic attachment and high adhesion coefficient

The growth angle of the setal branches to the surface is key .

Amonton’s first law states that the relationship of shear force or friction to the normal load is a constant value. We know it as μ or the coefficient of friction. Friction is therefore determined by the normal load. Setal arrays in Geckos do not grow perpendicularly to the surface of the toe pad but rather grow at a slight angle. Furthermore spatular branches grow almost perpendicularly to the long axis of the setal branches. Hence when setae are dragged across a surface against their natural curvature (the ‘non-adhesive’ direction), they do not adhere and instead exhibit typical Amonton’s friction since the non-branched tips of individual setal branches are in contact with the surface. See figure (14) on the next page.

In contrast, when dragged along their natural curvature, setae exhibit a response that violates Amontons' first law. Adhered setae maintain strong static and kinetic friction even while under tensile loading and adhesion is determined by friction. [6] As sheer stress on setal arrays increases setal branches bend so spatular branches are closer to the surface. At greater sheer loads more spatular tips are in direct contact with the surface and attachment force increases. The requirement of shear force in a specific direction to maintain adhesion is a great advantage because it provides precise control over adhesion by way of friction allowing strong and precisely controlled attachment.

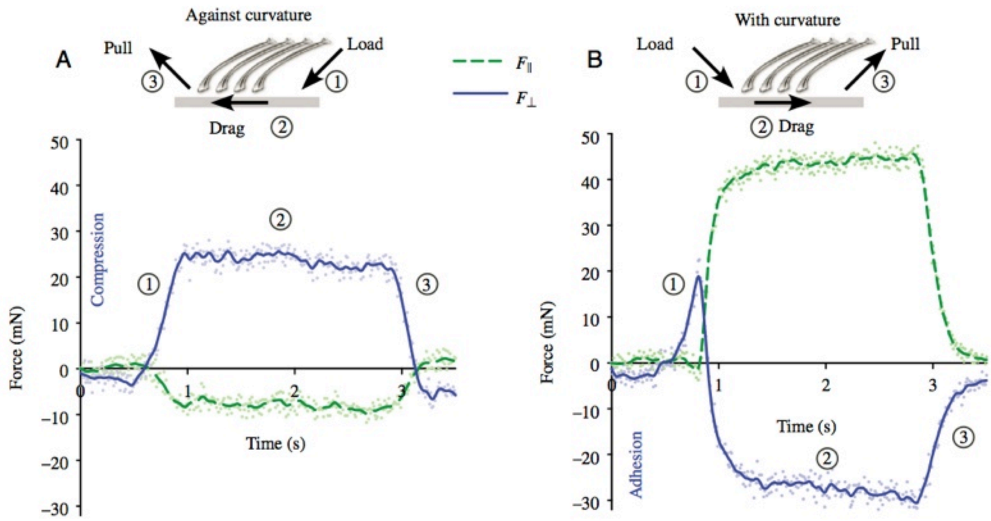

(14)

Force graphs showing adhesion and compression forces in a load,drag,pull sequence of a Gecko setal array in the tilted and untilted directions. [6]

5.4. Low detachment force

The effective stiffness of a setal arrays is low.

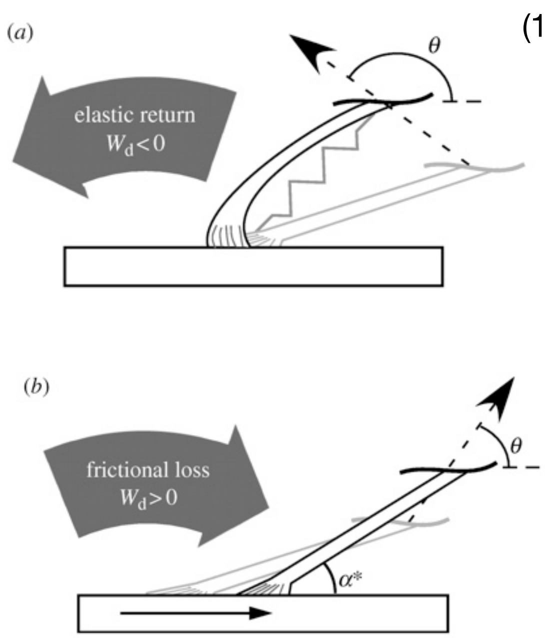

(15)

The requirement of shear force for adhesion is also responsible for low forces necessary for detachment. Experiments have shown that once shear stress decreases setal branches return to their non-adhesive positions and spatular branches release. I will now explain the fundamental principles that setal branches have to posses for this process to work properly.

Once a setal branches's angle to the surface exceeds 30º detachment occurs. Stress increases at the trailing edge of the seta causing fracture of the seta-substrate bonds and the seta returns to the unloaded default state. This scenario is supported by models of setae as cantilever beams. [6] The release of elastic energy stored in the setal shafts as the shaft angle to the surface increases helps the branched spatular nano-structure to de-adhere.

(a) During detachment along a 130° linear path, the setal tip remains stationary while the shaft unloads elastically, resulting in spontaneous debonding (W_d<0). (b) A largely proximal linear detachment path causes setae to remain in tension, inhibiting elastic energy return to the system. [14]

Geckos also lift up their toes in a peeling manner so individual setal branches release contact in rows rather than all at once. Not only is detachment force of individual setal branches low but the force necessary to achieve detachment can be stretched out over a period of time enabling detachment to be a controlled process.

5.5. Anti self-matting and non-sticky default state

Pressing 2 setal arrays together yields a small contact area. B-keratin is a non-tacky substance.

Conventional pressure sensitive adhesives (PSAs) are fabricated from soft viscoelastic materials that satisfy Dahlquist's criterion for tack with a Young's modulus (E) of 100 kPa or less at room temperature and 1 Hz. This criterion can be broadly described as a need for a material to be pliable in order to absorb energy inputs rather than allowing it to propagate through cracks. In contrast, the adhesive on the toes of geckos is made of ß-keratin, a stiff material with E at least four orders of magnitude greater than the upper limit of Dahlquist's criterion. Therefore, one would expect a setal array structure to not function as a PSA by deforming readily to make intimate molecular contact with a variety of surface profiles. However, since the gecko adhesive is a microstructure in the form of an array of millions of high aspect ratio shafts, the effective elastic modulus E_{eff} is much lower than E of bulk ß-keratin. The cantilever beam mechanical model of a setal array angled at 37^{o} calculates the E_{eff} at 100kPa which still qualifies as tacky. See figure (16) bellow. [7]

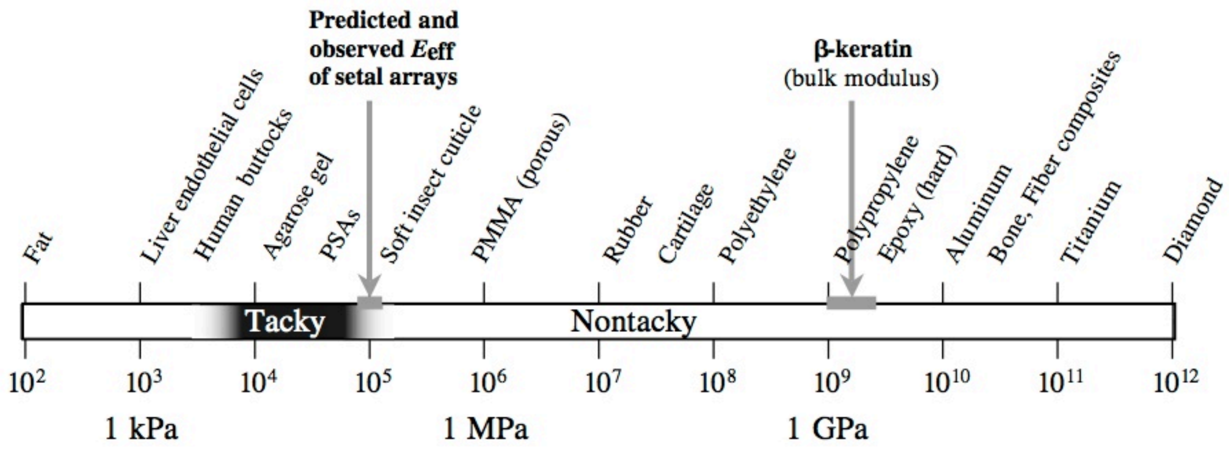

(16)

Youngs modulus, E(Pa) [8]

As explained in chapter 4.2 models suggest self-cleaning in fact requires surface energies of spatulae to be relatively low. Decreasing surface energy evidently decreases adhesion energy of each spatula to the surface but it promotes self-cleaning and anti-self mating at the same time. These 2 effects increase adhesion of the array as a whole by maximising the number of uncontaminated and unmated spatulae. [8] Another reason setal branches do not self-mate is the small contact area between spatular branches when 2 setal arrays are pressed together.

B-keratin being non-tacky is not the only reason setal arrays are non-sticky in their default state. Once an array comes into contact with a surface a very small portion of setal branches make contact since setal branches in an array are not perfectly lined up, the length of individual hair also differs and adhesion is hence limited. Only after preload (a small perpendicular force) and drag (a parallel pull) is applied the setal array makes closer contact with the surface, setal branches properly line up and a greater portion of them adhere to the surface. Calculations show that in order for the gecko to properly adhere the number of setal branches in contact after the pull and drag sequence must increase 7,5-fold. [8]

6. Effective models of Gecko Nano-structures

Using a nanostructure to create an adhesive is a novel and bizarre idea. It is possible that if it had not evolved in nature, humans would never have invented it. Gecko-like synthetic adhesives (GSAs) are under rapid development and with each generation more gecko-like properties will emerge.

But there is a lot more than scientifically curiosity driving the research in to GSAs. There are revolutionary ways we could put them to use. Since a nanostructure could be applied directly to a surface, it is conceivable that gecko-like structures could replace screws, glues and interlocking tabs in many assembly applications, such as automobile dashboards or mobile phones. Joints would have to be cleverly designed taking frictional adhesion into account. Easy disassembly for repair or recycling should be possible, self cleaning adhesive nano-structures could dramatically reduce our reliance on cleaning solvents and surface preparation, 2 processes that currently leave a big footprint on our environment. [6]

Revolutionary climbing and rescue suits as well as climbing robots could be developed, car tires with nano-structures applied to them are a novel concept while microelectromechanical systems and biomedical applications are already in the testing phase. I will conclude this seminar by presenting a few existing GSAs technologies and compare their properties with the 7 benchmark functional properties of naturally occurring gecko setae.

6.1. Synthetic polyimide pillar GSA

In the past few years a multitude of methods have been used to reproduce Gecko-like materials from polymers. Single strand vertical arrays of cylindrical pillars were produced by electron-beam lithography and tested at the University of Manchester in 2003. The method involved preparing a 5μm thin polyimide film on a silicon wafer. Then using electron-beam lithography and thermal evaporation of an aluminium film an array of sub-micrometer aluminium disks was prepared. The pattern of these disk was transferred to the polyimide base and dry etching with oxygen plasma was performed. Because of the large difference of etching rates of aluminium and polyimide a large portion of the polyimide could be etched away before the aluminium mask disappeared. The result was an array of vertical round shaped pillars. See figure (17).

Different pillar densities and pillar radius were produced and tested. A big problem was producing hairs flexible enough to attach to uneven surfaces but that do not break, curl or tangle. Examination in a scanning electron microscope (SEM) revealed that very thin pillars ($D < 0.3$ μm) tend to fall down, whereas long, closely spaced hairs tend to bunch after being in contact with the opposite surface. The optimal geometry eventually chosen was with hairs as long as they could be made ($H \approx 2$ μm), reasonably dense ($P \approx 1.6$ μm) and not too thin ($D \approx 0.5$ μm). [10]

(18)

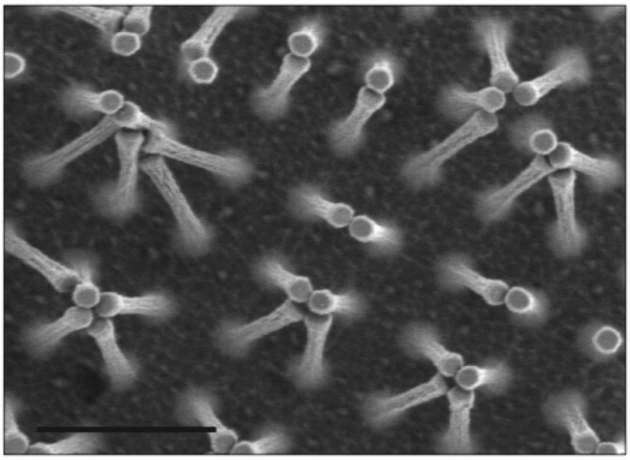 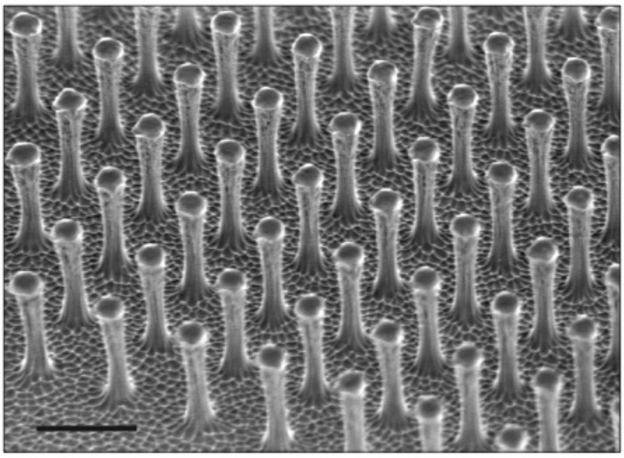 (17)

Bunching is found to be one of the mechanisms responsible for the reduction of adhesive strength of the artificial hair. The scal bar is are 2 µm long.[10]

A small area near the edge of a 1 cm2 array of polyimide hairs. The scal bar is are 2 µm long.[10]

Initial testing results were discouraging with small adhesive forces produced suggesting only 1% of the hairs were in contact with the surface. After applying the thin polyimide film with the pillar array to a soft bonding substrate adhesion improved by nearly 1000 times. The force produced though was found to be practically independent of the preload which suggested all of the hairs would attach to the surface simultaneously. The produced tape also showed isotropic attachment. The product was reusable but showed signs of decay over repeated use. The polyimide pillars tended to break of a permanently stick to the polyimide surface. Comparing this adhesive to the 7 benchmark properties of the Gecko system we can come to the following conclusions.

Material independence is shown to a degree but a soft polyimide base has to be used to achieve proper connection to the surface of all the pillars. The forces produced were $3N/cm^2$ compared to the $10N/cm^2$ of Gecko setae. The material was only partially non-self mating but it did have a non-sticky default state while it was not tested for self-cleaning. A lot was learned from these early experiments and in the next chapter I will explain the big advances that have been made learning from the setbacks of these early models.

6.2. Vertical and angled polydimethylsiloxane flaps

Many of the disadvantages found in vertical pillar arrays can be overcome by designing the array from flaps rather than pillars. In 2011 a paper called Gecko-Inspired Dry Adhesive for Robotic Applications was published exploring the characteristics of vertical and angled flaps from polydimethylsiloxane (PDMS). [11] The lateral force of friction is more important than adhesion in vertical climbing robot applications. A simple equation that describes the friction force between 2 adhesive surfaces is written bellow. See equation (18).

$$F_{||} = \mu F_{\perp} + S_c A_{real} \tag{18}$$

$F_{\perp}$ is the normal load, μ is the friction coefficient, S_c is the shear strength, and A_{real} is the real contact area. The first term is Amonton's law for non-adhering surfaces and it dominates at high loads. The second term is the adhesion dependant contribution which is proportional to the real molecular contact area and it dominates in Gecko adhesive systems. A major problem pillar arrays face is a small contact area with the surface. Micro-flap designs effectively increase contact area. Furthermore contact area and consequently adhesion forces increase especially when loaded perpendicularly and pulled in the adhesive direction of -/+y. See figure (19).

(19)

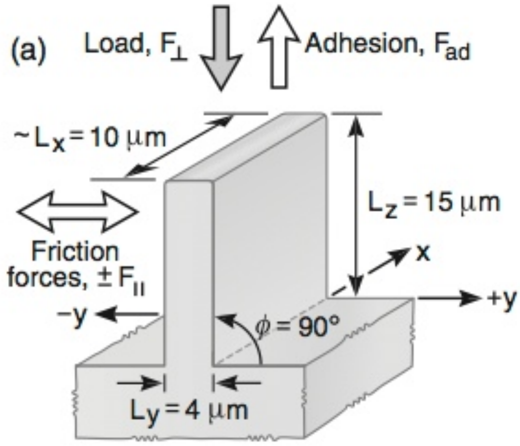

The width of the micro-flaps is about 2.5 times bigger than the thickness and therefore the stiffness along the smaller face of the flaps is much higher. Anisotropic stiffness of the PDMS micro-flaps being direction dependant is crucial to both the friction and adhesion properties of the vertical flaps. For a small deflection, assuming deformation is governed by small-deflection cantilever bending, the stiffness of a vertical flap is k. See equation (20).

$$I = \frac{bh^3}{12}; \quad k = \frac{3EI}{L^3} \tag{20}$$

E = 0.75 MPa is the elastic modulus of the cross-linked PDMS, L is the height of the flap, and I is the area moment of inertia. I can be calculated as shown in equation (20) where b is the width along the bending direction and h is the thickness in the bending direction.

Using the size of the vertical PDMS flaps fabricated, we can get $I_X = 0.333 \times 10^{-21}$ m^4 and $I_Y = 0.053 \times 10^{-21}$m^4. A single vertical flap is therefore 6 times stiffer in the ±x direction than in the ±y direction. Due to this higher stiffness, the flaps are hard to deform elastically in the ±x direction. The high stiffness also prevents a large contact area between the surface and the micro-flaps therefore reducing adhesion between surfaces, which would explain the pure load-controlled behaviour of friction when sliding along the ±x direction. The smaller stiffness along the large face makes the flaps easier to bend over during sliding, which increase contact area and thus causes adhesion controlled friction at low normal loads.[11]

Flaps angled at **Φ=70º** (figure) perform even more Gecko-like than vertical ones. The tilted angle gives rise to an anisotropic stiffness of the flaps. The stiffness of a flap with a tilted angle j under a normal load $F_\perp$ and a shear force $F_{||}$ could be estimated with equation (21). [11]

$$k = \frac{F_{||}}{\Delta_{approx}} = \frac{F_{||}}{\frac{L_z^3}{3EI}\left[F\perp cos^2(\phi) \pm F_{||}\, sin(\phi)cos(\phi)\right]} \tag{21}$$

In the above equation, take the positive sign if sheared in the direction of tilt (the +y direction), and negative if sheared in the opposite direction (the −y direction). This simple model predicts the anisotropic stiffness of the angled flaps: sliding against the direction of tilted direction gives higher stiffness, and sliding in the tilt direction results in lower stiffness. This direction dependent stiffness strongly affects the adhesion properties of the flaps. See figure (22).

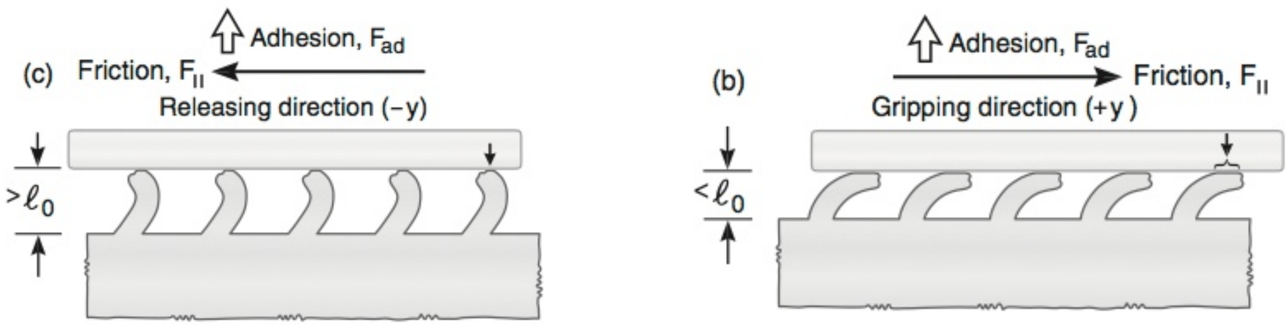

(22)

Schematic of the frictional adhesion mechanism of the angled flaps. [11]

In addition for only the normal adhesion test without shearing due to the top surface roughness of the flaps, the flaps only make point contacts with the glass surface. The small contact area results in small adhesion that is insensitive to preload. As we can see angled micro-flaps more closely mimic the naturally occurring Gecko setal arrays than their pillar counterparts thus their adhesive characteristics meet the 7 benchmark properties to a much greater degree.

6.3. Multi-walled carbon nanotube GSAs

There is another emerging method of forming Gecko like adhesives. Growing carbon nanotubes in bundles can produce results that mimic the setal as well as spatular characteristics of the Gecko setal array. See figure (23). Tapes with nanotubes applied to them have shown to produce 36N/cm^2 of sheer force compared to the natural Gecko spatular array that produces 10N/cm$^{2.}$ [11] For electronics, micro-electro-mechanical systems (MEMS) and cryogenic or high temperature environments, polymer based adhesives, including polymer GSAs, are not appropriate because of their low thermal and electrical conductivity. Polymers are also much less durable than carbon nanotubes. Carbon nanotube GSAs would be desirable for these application as they could serve as a dry adhesive with high electrical and thermal conductivity and high adhesion strengths while still being selectively detachable. Since carbon nanotube designs of GSAs closely mimic the Gecko's setal arrays self-cleaning has also been shown to happen. [13]

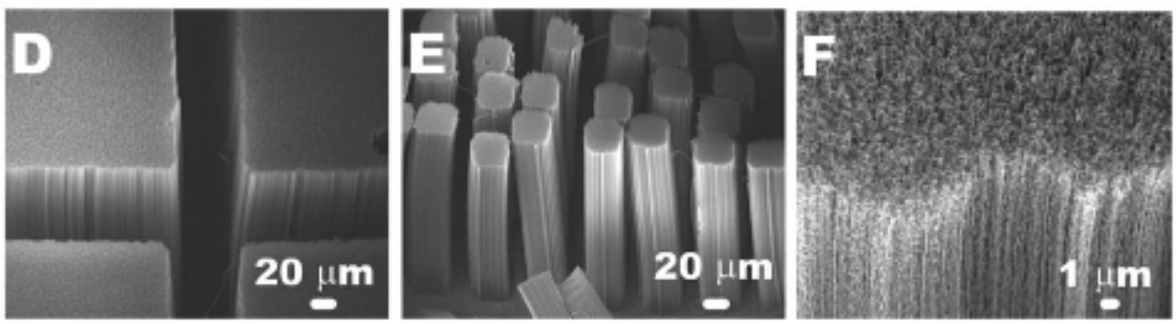

(23)

(D-E) SEM images of synthetic setae made of micropatterned carbon nanotube bundles of varying size. (F) Higher magnification SEM image of synthetic setae showing thousands of vertically aligned carbon nanotubes that act as spatulas [14]

7. Conclusion

The main advances in past years have been made by reproducing the angled nature of setal arrays thus promoting bending and effective elastic energy storage rather then bulking as is the case in vertically aligned arrays. [9] Achieving a branched structure with carbon nanotube designs is also a big breakthrough. As technology and insights in to the Gecko adhesive system advance forward we will be able to even more closely mimic the 7 benchmark functional properties described in chapter 4 of this seminar and GSAs may someday even exceed the properties of natural Gecko setal arrays.

8. References:

[1] Kellar Autumn, Metin Sitti§, Yiching A. Liang, Anne M. Peattie, Wendy R. Hansen, Simon Sponberg, Thomas W. Kenny, Ronald Fearing, Jacob N. Israelachvili, and Robert J. Full (2002) PNAS, vol.99, no19, 12253

[2] http://en.wikipedia.org/wiki/Van_der_Waals_force

[3] http://en.wikipedia.org/wiki/London_dispersion_force

[4] W. R. Hansen, and K. Autumn (2004) PNAS vol. 102, no. 2, 385/389

[5] Kellar Autumn, Yiching A. Liang2, S. Tonia Hsieh, Wolfgang Zesch, Wai Pang Chan, Thomas W. Kenny, Ronald Fearing & Robert J. Full3 (2000) Nature, vol. 405.

[6] Kellar Autumn and Nick Gravish (2008) Phil. Trans. R. Soc. A (2008) 366, 1575–1590

[7] K. Autumn1, C. Majidi, R. E. Groff2, A. Dittmore and R. Fearing (2006) The Journal of Experimental Biology 209, 3558-3568

[8] Kellar Autumn (2006) Properties, principles, and parameters of the gecko adhesive system. In Smith, A. and J. Callow, Biological Adhesives. Springer Verlag.

[9] http://robotics.eecs.berkeley.edu/~ronf/Gecko/index.html

[10] A. K. Geim, S. V. Dubons, I. V. Grigorieva1, K. S. Novoselov1, A. A. Zhukov and S. Yu. Shapoval (2003) nature materials | VOL 2

[11] Jing Yu, Sathya Chary, Saurabh Das, John Tamelier, Noshir S. Pesika, Kimberly L. Turner, and Jacob N. Israelachvili* (2011) Adv. Funct. Mater. 2011, XX, 1–9

[12] Liehui Ge, Sunny Sethi, Lijie Ci, Pulickel M. Ajayan, and Ali Dhinojwala (2007) PNAS vol. 104, no. 26, 10792–10795

[13] Sunny Sethi, Liehui Ge, Lijie Ci, P. M. Ajayan, and Ali Dhinojwala, (2007) Nano Letters

[14] Nick Gravish, Matt Wilkinson and Kellar Autumn (2008) J. R. Soc. Interface 2008 5, 339-348

[15] http://www-f1.ijs.si/~rudi/sola/seminar_gecko.pdf